DOI/10.1007/s10059-011-1010-x

Minireview

Molecules and Cells

The Role of Sphingosine 1-Phosphate in Migration of Osteoclast Precursors; an Application of Intravital Two-Photon Microscopy

Taeko Ishii, Yutaka Shimazu, Issei Nishiyama, Junichi Kikuta, and Masaru Ishii*

Sphingosine-1-phosphate (S1P), a biologically active lysophospholipid that is enriched in blood, controls the trafficking of osteoclast precursors between the circulation and bone marrow cavities via G protein-coupled receptors, S1PRs. While S1PR1 mediates chemoattraction toward S1P in bone marrow, where S1P concentration is low, S1PR2 mediates chemorepulsion in blood, where the S1P concentration is high. The regulation of precursor recruitment may represent a novel therapeutic strategy for controlling osteoclast-dependent bone remodeling. Through intravital multiphoton imaging of bone tissues, we reveal that the bidirectional function of S1P temporospatially regulates the migration of osteoclast precursors within intact bone tissues. Imaging technologies have enabled *in situ* visualization of the behaviors of several players in intact tissues. In addition, intravital microscopy has the potential to be more widely applied to functional analysis and intervention.

INTRODUCTION

Bone is a highly dynamic organ that is continuously turned over during growth, even in adults. During bone remodeling, homeostasis is regulated by the balance between bone formation by osteoblasts and bone resorption by osteoclasts (Harada et al., 2003; Teitelbaum et al., 2003). However, in pathological conditions such as osteoporosis, osteopetrosis, arthritic joint destruction, and bone metastasis, this equilibrium is disrupted. Since osteoclasts are excessively activated in osteolytic diseases, the inhibition of osteoclast function has been a major therapeutic strategy. Bisphosphonates, the most widely used group of anti-osteoporosis drugs, bind to hydroxyapatite, enter osteoclasts via endocytosis, and induce osteoclast apoptosis (Russell et al., 2007). Recently, the inactivation of osteoclasts, as opposed to their elimination, has generated interest as an alternative treatment strategy (Deal, 2009; Yasuda et al., 2005). One promising regulation point is the recruitment of osteoclast precursors. In addition to several chemokines that are known regulators of migration, including CXCL12 (Yu et al., 2003) and CX_3CL1 (Koizumi et al., 2009), we have shown that sphingosine 1-phosphate (S1P), a lysophospholipid abundant in the plasma, plays an important role as both a chemoattractant and a chemorepellent (Ishii et al., 2009; 2010). In this review, we summarize the bidirectional regulation of osteoclast precursor migration by S1P and briefly describe intravital bone imaging in living animals.

S1P and its receptors

S1P is a bioactive sphingolipid metabolite that regulates diverse biological functions including cell proliferation, motility, and survival (Cyster, 2005; Rivera et al., 2008; Rosen et al., 2005; 2007). Sphingolipids are essential plasma membrane constituents composed of a serine head group and one or two fatty acid tails. They are easily metabolized and converted to sphingosines, which are ATP-dependently phosphorylated by sphingosine kinases 1 and 2 (SPHK1 and SPHK2) in most cells, yielding S1P (Hannun et al., 2008). SPHKs, which are regulated by a variety of growth factors, hormones, and cytokines, control S1P's acute reactive generation and homeostasis in the circulation (Hannun et al., 2008). Immediately after its synthesis, free S1P is irreversibly degraded by intracellular S1P lyase or dephosphorylated by S1P phosphatases. As a result, the levels of S1P in most tissues, including bone marrow, are relatively low. In contrast, large amounts of S1P are continuously produced in the plasma, especially by erythrocytes, and the serum concentration of S1P is extremely high (several hundred nanomolar to low-micromolar range). Most S1P in the circulation is bound to high-density lipoprotein (HDL) and albumin, which serve as stable reservoirs and efficiently deliver S1P to epithelial cell-surface receptors (Argraves et al., 2008). In addition, because S1P is an amphiphilic molecule that cannot easily cross membranes, an S1P gradient between the blood and tissues is maintained.

S1P signals via five 7-transmembrane receptors or G protein-coupled receptors (GPCRs), S1PR1 to S1PR5, previously referred to as endothelial differentiation gene (Edg) receptors (Rivera et al., 2008; Rosen et al., 2007). Because of the different distribution of these receptors and their different coupling to signal-transducing G proteins, S1P shows a broad range of

Laboratory of Biological Imaging, WPI-Immunology Frontier Research Center, Osaka University, Osaka, Japan
*Correspondence: mishii@ifrec.osaka-u.ac.jp

Received January 13, 2011; accepted January 31, 2011; published online February 25, 2011

Keywords: cell dynamics, chemokine, chemotaxis, lipid mediator, live imaging

Table 1. S1P receptors and phenotypes of their genetic deletion

S1P Receptors	S1PR1	S1PR2	S1PR3	S1PR4	S1PR5
Coupling G proteins	$G_{i/O}$	G_i G_q G_s $G_{12/13}$	G_i G_q G_s $G_{12/13}$	G_i $G_{12/13}$	$G_{i/o}$ $G_{12/13}$
Distribution	Ubiquitous	Ubiquitous Highest expressed in embryonic brain Expressed high in adult heart and lung	Spleen, heart, lung, thymus, kidney, testis, brain, skeletal muscle	Thymus, spleen, lung, peripheral leukocytes	Brain, spleen, peripheral leukocytes
Phenotypes of gene deletion (mouse)	Embryonic lethal (e12.5-e14.5)	Vestibular defects Hearing loss Seizures (C57BL/6 only) Perinatal lethal (reduce litter size) Survivours show no phonotype	Disruption of alveolar epithelial junctions	Ddisorder of mega-karyocyte differentiation	Reduced number of NK cells
Biological function	Rac activation	Rho activation Vasoconstriction angiogenesis Wound healing	Cardioprotection by HDL		
References	Liu et al. (2000) Matloubian et al. (2004)	Kono et al. (2007) Serriere-Lanneau et al. (2007)	Nofer et al. (2004) Gon et al. (2005)	Golfier et al. (2010)	Walzer et al. (2007)

Cyster et al. (2005), Rivera et al. (2008), Rosen et al. (2005; 2007).

bioactivities (Table 1). S1PR1 is ubiquitously expressed and primarily coupled to PTX-sensitive $G_{i/o}$ proteins, whereas S1PR2 and S1PR3, whose distributions are more limited, are coupled to $G_{12/13}$ as well as G_q, G_s, and G_i. The expression of S1PR4 and S1PR5 is much lower than that of S1PR1, S1PR2, and S1PR3, and their functions remain to be elucidated. However, it has been reported that they are coupled to $G_{i/o}$ and $G_{12/13}$.

S1P receptors have key roles in the regulation of cellular motility. S1PR1 activates Rac through Gi and promotes cell migration and intercellular connection, whereas S1PR2 activates Rho signaling via $G_{12/13}$, thereby counteracting the effects of S1PR1 and inhibiting Rac activity (Takuwa, 2002). These differences account for the different biological functions of S1PR1 and S1PR2, which produce opposite effects on migration toward/against S1P gradients *in vitro* (Okamoto et al., 2000).

Osteoclast precursors and S1P

Osteoclasts are derived from macrophage/monocyte-lineage cells that express both S1PR1 and S1PR2 (Ishii et al., 2009). As described above, S1PR1 and S1PR2 have opposite effects on the migration of osteoclast precursors. Osteoclast precursors are chemoattracted to S1P *in vitro*, a response that is blocked by PTX. In addition, treatment with S1P increases osteoclast precursor levels of the active form of Rac (GTP-Rac), suggesting that Rac and Gi are involved in S1PR1 chemotactic signaling in osteoclast precursors. On the other hand, S1PR2 requires a higher concentration of S1P for activation and induces negative chemotactic responses, "chemorepulsion," to S1P gradients. S1PR2 activation causes cells to move from the bloodstream into bone marrow cavities (Ishii et al., 2010). As in leukocytes, the migration of osteoclast precursors is regulated by chemokines. Like the S1PRs, chemokine receptors are GPCRs and signal via Gi components. One of the best-known chemoattractants for osteoclast precursors is CXCL12 (also known as stromal derived factor-1), a CXCR4 ligand (Yu et al., 2003). CXCL12 is constitutively expressed at high levels by osteoblastic stromal cells and vascular endothelial cells in bone, whereas CXCR4 is expressed on a wide variety of cells types, including circulating monocytes and osteoclast precursors. CXCL12 has chemotactic effects on osteoclast precursors, which express large amounts of CXCR4.

Recently, another chemokine, CX_3CL1 (also known as fractalkine), which functions as a membrane-bound adhesion molecule, was shown to act as a chemoattractant after its cleavage by ADAM10 and ADM7. Expressed by osteoblastic stromal cells, it was reported to be involved in both the recruitment and attachment of osteoclast precursors (Koizumi et al., 2009). Expression of both chemokine receptors and S1PRs is reduced by RANKL stimulation, dependent on NF-κB, but not on NF-AT. Presumably, after cells mature and arrive at their ultimate destinations these chemoattractants are no longer needed.

Application of intravital imaging to the analysis of cell behavior in bone

To study the behavior of osteoclasts and their precursors *in vivo*, we developed a new intravital two-photon imaging system for use in the analysis of bone tissues (Fig. 1) (Ishii et al., 2009; 2010). Recent advances in microscope, laser, and fluorophore technology have made it possible to visualize living cells in intact organs and to analyze their mobility and interactions in a quantitative manner.

As calcium phosphate, the main structural component of the bone matrix, can scatter laser beams, it was difficult to access the deep interior of bone tissues, even using a near-infrared laser. We decided to use parietal bone in which the distance from the bone surface to the bone marrow cavity is 80-120 μm (within the appropriate range for two-photon microscopy). We

Fig. 1. Bone marrow structure visualized by intravital two-photon imaging. Murine skull bone tissues of heterozygous Cx_3CR1-EGFP knock-in mice. Collagen fibers in bone are detected by second-harmonic generation (in blue), and the microvasculature are visualized by intravenous injection of 70 kDa dextran-conjugated Texas Red. CX_3CR1-EGFP positive cells appear green in bone marrow cavity.

modified the method used in a pilot study, which revealed that central memory $CD8^+$ T cells were preferentially recruited to, and accumulated in, the bone marrow cavity and interacted with mature circulating dendritic cells (Cavanagh et al., 2005; Mazo et al., 2005).

Using this new intravital two-photon imaging method, we showed that S1P controls the migratory behavior of osteoclast precursors, dynamically regulating bone mineral homeostasis, and we identified a critical control point in osteoclastogenesis. While monocytoid cells containing osteoclast precursors (CSF1R-EGFP-positive or CX3CR1-EGFP-positive cells) were stationary at the steady state, osteoclast precursors were stimulated and moved into vessels when a potent S1PR1-specific agonist, SEW2871 (Wei et al., 2005), was injected intravenously.

To clarify the physiological significance of S1P-directed chemotaxis of osteoclast precursors in bone homeostasis, we examined osteoclast/monocyte-specific S1PR1-deficient ($S1PR1^{-/-}$) mice. [Global S1PR1 deficiency causes embryonic lethally at e12.5 to e14.5 due to defective blood vessel development (Liu et al., 2000)]. The attachment of osteoclast precursors to bone surfaces was significantly enhanced in $S1PR1^{-/-}$ animals compared with controls. $S1PR1^{-/-}$ osteoclasts precursors on bone surfaces subsequently develop into mature osteoclasts and absorb bone tissues. S1P-mediated chemotaxis of osteoclast precursors would thus be expected to contribute to their redistribution from bone tissues to blood vessels.

We also performed intravital two-photon imaging of bone tissues to define the role of S1PR2 *in vivo* (Ishii et al., 2010). We showed that certain osteoclast precursors (CX_3CR1-EGFP-positive cells) moved into the bloodstream when a potent S1PR2 antagonist, JTE013 (Osada et al., 2002), was injected intravenously. The effect of JTE013 was less pronounced than that of the S1PR1 agonist SEW2871. Furthermore, to clarify the physiological significance of $S1P^{-/-}$ chemotaxis of osteoclast precursors in bone homeostasis, we examined S1PR2-deficient ($S1PR2^{-/-}$) mice. Although $S1PR2^{-/-}$ mice suffer auditory impairment due to vessel defects in the inner ear, they survive and reproduce (Kono et al., 2007). Although bone resorption of osteoclasts was significantly lower in $S1PR2^{-/-}$ animals than in controls, *in vitro* osteoclast formation was not significantly affected. In a high-S1P environment such as the bloodstream, S1PR1 is activated and rapidly internalized, allowing S1PR2 to predominate. Osteoclast precursors enter the bone marrow as a result of chemorepulsion mediated by S1PR2, and other chemo-

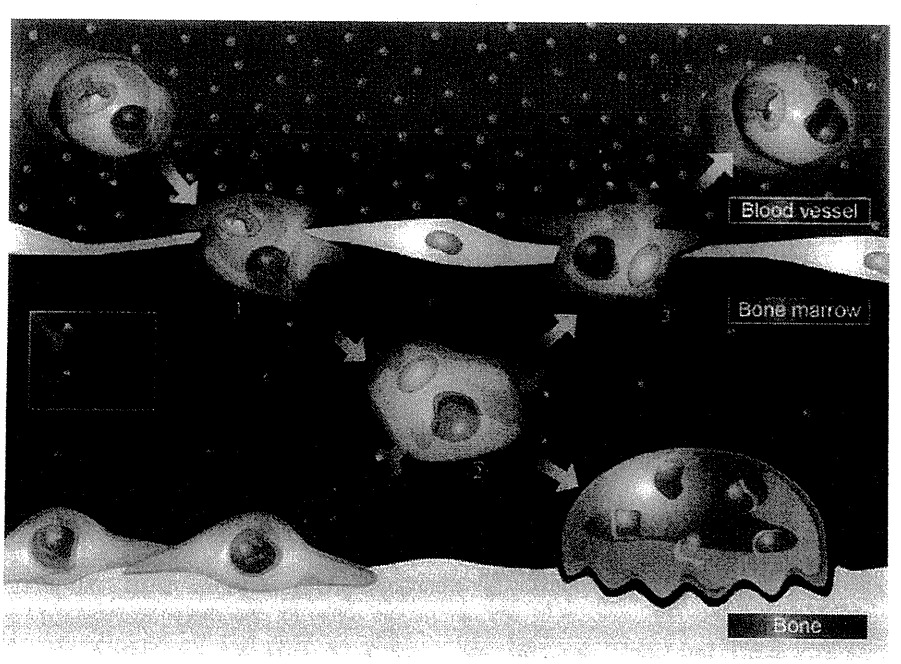

Fig. 2. A schematic model for S1P-mediated osteoclast precursors localization. The entry of osteoclast precursors from blood vessels where S1P is at high concentration, is initiated by chemorepulsion through S1PR2 (1). Once enter in bone marrow, osteoclast precursors migrate toward chemokines enriched in bone marrow cavity (2). On the other hand, their recirculation toward blood vessels is regulated by chemoattraction through S1PR1 (3).

kines attract them to bone surfaces. After they enter a low-S1P environment such as bone marrow, S1PR1 is transported back to the cell surface, and osteoclast precursors return from bone tissues to blood vessels as a result of chemotaxis to an S1P gradient.

The number of osteoclast precursors on bone surfaces is determined by the balance between the trafficking of osteoclast precursors to and from the circulation. These data provide evidence that S1P controls the migratory behavior of osteoclast precursors, dynamically regulating bone mineral homeostasis, and identify a critical control point in osteoclastogenesis. Based on our findings, we propose that regulation of the migratory behavior of osteoclast precursors controls osteoclast differentiation. This control mechanism is summarized in Fig. 2. This critical control point in osteoclastogenesis may represent an attractive target for new treatments for osteoporosis. We previously showed that treatment with FTY720, which is metabolized by SPHK2 to a compound that acts as an agonist for four of the five S1P receptors (not S1PR2) (Cyster, 2005; Matloubian et al., 2004), relieved ovariectomy-induced osteoporosis in mice by reducing the number of mature osteoclasts attached to bone surfaces (Ishii et al., 2009). The mechanism of action of S1P is completely different from that of conventional treatments such as bisphosphonates, which suppress mature osteoclasts. We anticipate that the regulation of osteoclast precursor migration may be a useful clinical strategy in the near future.

FTY720 is a reversible immunosuppressive agent approved as a treatment for multiple sclerosis in the United States. It induces lymphopenia by confining lymphocytes to lymphoid organs (Mandala et al., 2002). The precise mechanisms behind this phenomenon remain controversial, and it is necessary to determine how FTY720 produces the opposite effect on monocyte-macrophage cells in bone marrow (which are expelled into the circulation by FTY720).

Future directions for two-photon microscopy

Two-photon intravital imaging has revealed, and continues to reveal, dynamic features of physiological and pathological process. Its greatest strength is its ability to provide spatiotemporal information in living organisms, which cannot be achieved using other methods. However, current two-photon microscopy imaging techniques have several limitations. First, we cannot see everything in the visual fields in two-photon microscopy. Although fluorescence labeling and second-harmonic generation enable us to observe target cells and organs, the lack of a signal does never reflect an open field, as diverse structures and cellular components should be present. To avoid misinterpretation, we must interpret our observations with caution. Second, although two-photon microscopy has greater penetration depth than conventional confocal microscopy, its penetration depth is only 800-1000 μm in soft tissues (e.g., brain cortex) and 200 μm in hard tissues (e.g., bone). Because of these resolution limitations, it may only be applied to small animals, such as mice and rats. Moreover, due to the wide scattering of light by the skin, it is necessary that target organs should be exteriorized. It is possible that the necessary operative invasion and changes in oxygen concentration and humidity may influence cellular behavior. To resolve these problems, technical innovations in fluorochrome and optical systems, including improvements in light emission and amelioration of resolution problems (Ntziachristos, 2010), are needed.

Intravital microscopy has begun to be applied not only to observational studies, but also to functional analysis and interventions. Recently, several new fluorescence tools have been developed. These include cell-cycle indicators (Sakaue-Sawano et al., 2008) and light-sensing devices such as photoactivatable fluorescent proteins (Victora et al., 2010) and light-induced activators of G protein-coupled receptors (Airan et al., 2009).

CONCLUSION

As the recruitment of osteoclast precursors during osteoclastogenesis is dynamic and dependent on the microenvironment of the bone marrow cavity, temporospatial information is very important. Intravital imaging has made a huge contribution to improving our understanding of these processes. It enables us to visualize, temporospatially, complicated systems in living organisms. This new technique has revealed that S1P acts in concert with several chemoattractants to shepherd osteoclast precursors to appropriate sites. Controlling the recruitment and migration of osteoclast precursors represents a promising new therapeutic strategy for combating bone diseases. Although their limitations remain to be resolved, the range of applications for *in vivo* imaging techniques continues to expand.

REFERENCES

Airan, R.D., Thompson, K.R., Fenno, L.E., Bernstein, H., and Deisseroth, K. (2009). Temporally precise *in vivo* control of intracellular signalling. Nature *458*, 1025-1029.

Argraves, K.M., Gazzolo, P.J., Groh, E.M., Wilkerson, B.A., Matsuura, B.S., Twai, W.O., Hammad, S.M., and Argraves, W.S. (2008). High density lipoprotein-associated sphingosine 1-phosphate promotes endothelial barrier function. J. Biol. Chem. *283*, 25074-25081.

Cavanagh, L.L., Bonasio, R., Mazo, I.B., Halin, C., Cheng, G., van der Velden, A.W., Cariappa, A., Chase, C., Russell, P., Starnbach, M.N., et al. (2005). Activation of bone marrow-resident memory T cells by circulating antigen-bearing dendritic cells. Nat. Immunol. *6*, 1029-1037.

Cyster, J.G. (2005). Chemokines, sphingosine-1-phosphate, and cell migration in secondary lymphoid organs. Annu. Rev. Immunol. *23*, 127-159.

Deal, C. (2009). Future therapeutic targets in osteoporosis. Curr. Opin. Rheumatol. *4*, 380-385.

Golfier, S., Kondo, S., Schulze, T., Takeuchi, T., Vassileva, G., Achtman, A.H., Gräler, M.H., Abbondanzo, S.J., Wiekowski, M., Kremmer, E., et al. (2010). Shaping of terminal megakaryocyte differentiation and proplatelet development by sphingosine-1-phosphate receptor S1P4. FASEB J. *24*, 4701-4710.

Gon, Y., Wood, M.R., Kiosses, W.B., Jo, E., Sanna, M.G., Chun, J., and Rosen, H. (2005). S1P3 receptro-induced reorganization of epithelial tight junctions compromises lung barrier integritiy and is potentiated by TNF. Proc. Natl. Acad. Sci. USA *102*, 9270-9275.

Hannun, Y.A., and Obeid, L.M. (2008). Principles of bioactive lipid signaling: lessons from sphingolipids. Nat. Rev. Mol. Cell. Biol. *9*, 139-150.

Harada, S., and Rodan, G.A. (2003). Control of osteoblast function and regulation of bone mass. Nature *423*, 349-355.

Ishii, M., Egen, J.G., Klauschen, F., Meier-Schellersheim, M., Saeki, Y., Vacher, J., Proia, R.L., and Germain, R.N. (2009). Sphingosine-1-phosphate mobilizes osteoclast precursors and regulates bone homeostasis. Nature *458*, 524-528.

Ishii, M., Kikuta, J., Shimazu, Y., Meier-Schellersheim, M., and Germain, R.N. (2010). Chemorepulsion by blood S1P regulates osteoclast precursor mobilization and bone remodeling *in vivo*. J. Exp. Med. *207*, 2793-2798.

Koizumi, M., Saitoh, Y., Minami, T., Takeno, N., Tsuneyama, K., Miyahara, T., Nakayama, T., Sakurai, H., Takano, Y., Nishimura, M., et al. (2009). Role of CX3CL1/fractalkine in osteoclast differentiation and bone resorption. J. Immunol. *183*, 7825-7831.

Kono, M., Belyantseva, I.A., Skoura, A., Frolenkov, G.I., Starost, M.F., Dreier, J.L., Lidngton, D., Bolz, S.S., Friedman, T.B., Hla, T., et al. (2007). Deafness and stria vascularis defects in S1P2 receptor-null mice. J. Biol. Chem. *282*, 10690-10696.

Liu, Y., Wada, R., Yamashita, T., Mi, Y., Deng, C.X., Hobson, J.P., Rosenfeldt, H.M., Nava, V.E., Chae, S.S., Lee, M.J., et al.

(2000). Edg-1, the G-protein-coupled receptor for sphingosine-1-phosphate, is essential for vascular maturation. J. Clin. Invest. *106*, 951-961.

Mandala, S., Hajdu, R., Bergstrom, J., Quackenbush, E., Xie, J., Milligan, J., Thornton, R., Shei, G.J., Card, D., Keohane, C., et al. (2002). Alteration of lymphocyte trafficking by sphingosine-1-phosphate receptor agonists. Science *296*, 346-349.

Matloubian, M., Lo, C.G., Cinamon, G., Lesneski, M.J., Xu, Y., Brinkmann, V., Allende, M.L., Proia, R.L., and Cyster, J.G. (2004). Lymphocyte egress from thymus and peripheral lymphoid organs is dependent on S1P receptor 1. Nature *6972*, 355-360.

Mazo, I.B., Honczarenko, M., Leung, H., Cavanagh, L.L., Bonaisio, R., Weninger, W., Engelke, K., Xia, L., McEver, R.P., Koni, P.A., et al. (2005). Bone marrow is a major reservoir and site of recruitment for central memory CD8+ T cells. Immunity *22*, 259-270.

Nofer, J.R., van der Giet, M., Tolle, M., Wolinska, I., von Wnuck Lipinski, K., Baba, H.A., Tietge, U.J., Godecke, A., Ishii, I., Kleuser, B., et al. (2004). HDL induces NO-dependent vasorelaxation via the lysophospholipid receptor S1P3. J. Clin. Invest. *113*, 569-581.

Ntziachristos, V. (2010). Going deeper than microscopy: the optical imaging frontier in biology. Nat. Methods *7*, 603-614.

Okamoto, H., Takuwa, N., Yokomizo, T., Sugimoto, N., Sakurada, S., Shigematsu, H., and Takuwa, Y. (2000). Inhibitory regulation of Rac activation, membrane ruffling, and cell migration by the G protein-coupled sphingosine-1-phosphate receptor EDG5 but not EDG1 or EDG3. Mol. Cell. Biol. *20*, 9247-9261.

Osada, M., Yatomi, Y., Ohmori, T., Ikeda, H., and Ozaki, Y. (2002). Enhancement of sphingosine 1-phosphate-induced migration of vascular endothelial cells and smooth muscle cells by an EDG-5 antagonist. Biochem. Biophys. Res. Commun. *299*, 483-487.

Rivera, J., Proia, R.L., and Olivera, A. (2008). The alliance of sphingosine-1-phosphate and its receptors in immunity. Nat. Rev. Immunol. *8*, 753-763.

Rosen, H., and Goetzl, E.J. (2005). Sphingosine 1-phosphate and its receptors: an autocrine and paracrine network. Nat. Rev. Immunol. *5*, 560-570.

Rosen, H., Sanna, M.G., Cahalan, S.M., and Gonzalez-Cabrera, P.J. (2007). Tipping the gatekeeper: S1P regulation of endothelial barrier function. Trends Immunol. *28*, 102-107.

Russell, R.G.G., Xia, Z., Dunford, J.E., Oppernann, U., Kwaasi, A., Hulley, P.A., Kavanagh, K.L., Triffitt, J.T., Lundy, M.W., Phipps, R.J., et al. (2007). Bisphosphonates. An update on mechanisms of action and how these relate to clinical efiicacy. Ann. N Y Acad. Sci. *1117*, 209-257.

Sakaue-Sawano, A., Kurokawa, H., Morimura, T., Hanyu, A., Hama, H., Osawa, H., Kashiwagi, S., Fukami, K, Miyata, T., Miyoshi, H., et al. (2008). Visualizing spatiotemporal dynamics of multicellular cell-cycle progression. Cell *132*, 487-498.

Serrier-Lanneau, V., Teixeira-Clerc, F., Li, L., Schippers, M., de Wris, W., Julien, B., Tran-Van-Nhieu, J., Manin, S., Pelstra, K., Chun J., et al. (2007). The sphingosine 1-phosphate receptor S1P2 triggers hepatic wound healing. FASEB J. *21*, 2005-2013.

Takuwa, Y. (2002). Subtype-specific differential regulation of Rho family G proteins and cell migration by the Edg family sphingosine-1-phosphate receptors. Biochem. Biophys. Acta *1682*, 112-120.

Teitelbaum, S.L., Ross, F.P. (2003). Genetic regulation of osteoclast development and function. Nat. Rev. Genetic. *4*, 638-649

Victora, G.D., Schwichkert, T.A., Fooksman, D.R., Kamphorst, A.O., Meyer-Hermann, M., Dustin, M.L., and Nussenzweig, M.C. (2010). Germinal center dynamics revealed by multiphoton microscopy with a photoactivatable fluorescent reporter. Cell *143*, 592-605

Wei, S.H., Rosen, H., Matheu, M.P., Sanna, M.G., Wang, S.K., Jo, E., Wong, C.H., Parker, I., and Cahalan, M.D. (2005). Sphingosine 1-phospate type 1 receptor agonism inhibits transendothelial migration of medullary T cells to lymphatic sinuses. Nat. Immunol. *12*, 1228-1235.

Yasuda, Y., Kaleta, J., and Bromme, D. (2005). The role of cathepsins in osteoporosis and arthritis: rationale for the design of new therapeutics. Adv. Drug. Deliv. Rev. *57*, 973-993.

Yu, X., Huang, Y., Collin-Osdoby, P., and Osdoby, P. (2003). Stromal cell-derived factor-1 (SDF-1) recruits osteoclast precursors by inducing chemotaxis, matrix metalloproteinase-9 (MMP-9) acrivity, and collagen transmigration. J. Bone Miner. Res. *18*, 1404-1418.

SUPPLEMENT

How do contemporary imaging techniques contribute to basic and clinical rheumatology?

Masaru Ishii[1,2]

[1]Laboratory of Cellular Dynamics, WPI-Immunology Frontier Research Center, Osaka University, Osaka, Japan
[2]Japan Science and Technology Agency, CREST

Correspondence to
Masaru Ishii, Laboratory of Cellular Dynamics, WPI-Immunology Frontier Research Center, Osaka University, 3-1 Yamada-oka, Suita, Osaka 565-0871, Japan; mishii@ifrec.osaka-u.ac.jp

Received 10 August 2011
Accepted 25 September 2011

ABSTRACT

Recent major advances in biomedical imaging techniques have allowed us to visualise a variety of previously unseen biological phenomena. In particular, advanced fluorescent microscopy and radioimaging have enabled us to visualise cellular and molecular dynamics in living animals and humans. These new technologies have identified novel therapeutic targets against a wide array of diseases and have provided novel diagnostic tools for the evaluation of several disease conditions. In this brief review, the author outlines the contemporary imaging techniques used in the fields of immunology and rheumatology, with special focus on intravital fluorescent microscopy, and discusses how these cutting-edge methodologies contribute to clinical practice for patients with rheumatism.

Immune systems are highly dynamic, and the proper migration and localisation of relevant cell types are critically important for the maintenance of immune reactions. Classical analyses such as histological sectioning provide merely a snapshot of cellular localisation and molecular distribution but cannot provide temporal information. Recent advances in biological imaging techniques have revolutionised the biomedical sciences, and researchers can now obtain spatiotemporal information about the immune and inflammatory systems.

Here, the recently developed cutting-edge technology in optical microscopic imaging systems for the detection of cellular dynamics in intact tissues and organs, such as intravital multiphoton microscopy, is briefly introduced, and the findings closely related to the fields of rheumatology and immunology that could be discovered by this novel methodology are discussed. The possible use of radioimaging techniques for the evaluation of human immune systems is also described. Based on these technical advancements, the ways in which this new trend in biomedical sciences could contribute to the development of a new era in clinical rheumatology is discussed.

Intravital multiphoton imaging: a revolutionary tool for immunological studies

Recent advances in fluorescent microscopic techniques have revolutionised biological sciences; among them, the development and improved usability of two-photon excitation microscopy have enabled us to visualise biological phenomena that cannot be seen with conventional methods, such as the dynamic behaviour of cells deep inside living organs. In conventional fluorescent microscopy, a fluorophore absorbs energy from a single photon and then releases the energy as an emission photon. In multiphoton (normally two-photon) excitation mode, a fluorophore absorbs multiple photons simultaneously. This non-linear optical process can occur only in areas with extremely high photon density, such as the focal plane of optical paths. The limited excitation enables us to acquire bright and high-resolution images in regions deep inside tissues and organs. Near-infrared lasers used for multiphoton excitation can penetrate deeper, with less absorption or scattering, than the visible light used with confocal microscopy. Thus, objects can be visualised at depths of 100–1000 μm with two-photon excitation (table 1), whereas conventional imaging modalities such as confocal microscopy can only access areas at depths of less than 100 μm.[1] This property is beneficial for the analysis of live biological systems. The cells observed in a fixed and thin-sectioned sample are dead and no longer moving. The intravital visualisation of live dynamic systems often requires the observation of areas deep below the surface, which can only be achieved by two-photon excitation microscopy. Moreover, multiphoton excitation with near-infrared light can minimise photo bleaching and phototoxicity, thereby reducing damage to the imaged tissues and organs.[2 3]

Intravital multiphoton imaging has revolutionised biological research, especially in the field of immunology, where the cells comprising various immune tissues and organs are dynamic. For example, dynamic observations in lymph nodes have revealed the migratory changes in T cells in close contact with antigen-presenting dendritic cells.[4–6] When T cells encounter antigen-bearing dendritic cells, they form stable contacts lasting for at least several hours for priming and thereafter regain motility for recirculation. In thymic organ cultures, intravital imaging has shown interactions between thymocytes and stromal cells during positive and negative selection.[7] Live imaging has been tested for the visualisation of immune cell inflammatory reactions in many other tissues, such as those in the skin,[8] the lungs,[9] the liver[10] and the small intestine,[11] and has revealed various critical biological phenomena in each system.

The bone is a mineralised hard tissue that limits the passage of visible or infrared lasers, and it has long been considered to be extremely difficult to observe intact bone tissues in living animals.[12] We have developed a novel imaging system for visualisation inside bone cavities with high spatiotemporal resolution (figure 1). By using this technique, we can demonstrate that osteoclasts and their precursors migrate and localise under the control of several chemokines

Table 1 Comparison of optical imaging and radioimaging for studying medical sciences

	Optical imaging (multiphoton microscopy)	Radioimaging (positron emission tomography)
Spatial resolution	High (~1–10 μm)	Low (~1–10 mm)
Temporal resolution	High (0.1–10 s)	Low (10–30 min)
Visual field	Narrow (100–1000 μm)	Wide (100–2000 mm)
Depth of imaged areas	Shallow (100–1000 μm)	Deep (~1000 mm)
Multi-colour labelling	Possible	Impossible
Possible application for clinical rheumatology	- Revealing rapid cellular dynamics at local sites of inflammation (migratory behaviour, cell–cell interaction, etc)	- Revealing subacute/chronic changes of inflammation in total body (accumulation of immune cells and inflammatory molecules, etc)
	- Can only visualise the areas adjacent to the surface (eg, skin inflammation)	- Can visualise the events occurring deep inside the body
	- But can detect deeper areas with endoscope approaches (eg, gastrointestinal tracts, abdomen and joints)	- Spatiotemporal resolution is limited

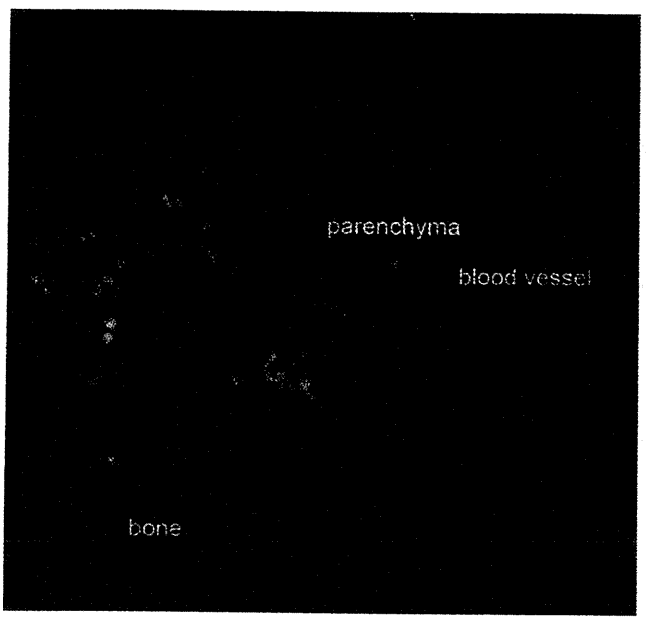

Figure 1 Stereoscopic view of bone marrow cavity visualised by intravital multiphoton imaging. Intravital imaging of the bone surface using multiphoton microscopy using CX_3CR1 promoter-driven EGFP-expressing mice. Blood vessels (red) and bone tissues (blue) were visualised by Texas Red-conjugated high-molecular dextrans (70 kDa) and second harmonic generation, respectively. Scale bars represent 30 μm.

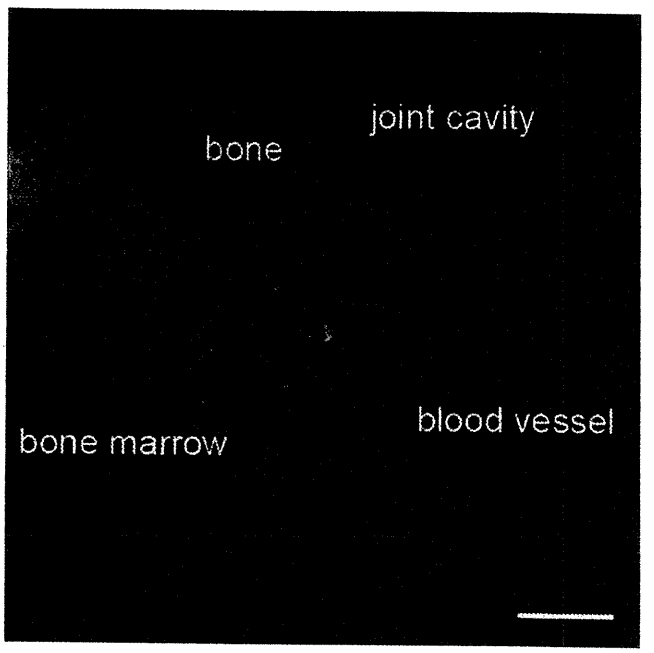

Figure 2 Intravital multiphoton imaging of a murine finger joint. Intravital imaging of a murine finger joint using multiphoton microscopy using LysM promoter-driven EGFP-expressing mice. Blood vessels (red) and bone tissues (blue) were visualised by Texas Red-conjugated high-molecular dextrans (70 kDa) and second harmonic generation, respectively. Scale bars represent 50 μm.

and lipid mediators, such as sphingosine-1-phosphate and CXC chemokine ligand 12.[13–15] Recently, we also successfully visualised the bone-resorbing activity of mature osteoclasts lining bone surfaces and identified their real mode of action in situ (manuscript submitted). Despite its hardness, the bone is a dynamic and elastic tissue that undergoes continuous remodelling by bone-resorbing osteoclasts and bone-replenishing osteoblasts. Inflammation and hormonal perturbation lead to the aberrant activation of osteoclasts, resulting in several bone-resorptive disorders, chiefly osteoporosis and rheumatoid arthritis (RA). Thus, osteoclasts have emerged as a good therapeutic target against these diseases, and the intravital imaging of bone tissues would be a good tool for the identification of novel target molecules and the development and evaluation of novel therapeutics.

USABILITY OF INTRAVITAL FLUORESCENT IMAGING TO REVEAL RA PATHOGENESIS

Intravital imaging is considered to be difficult because joints are surrounded by hard bone tissues and their structure is anatomically complex. To date, in vivo whole-body imaging with near-infrared optics has been used to detect inflammation in murine arthritic models,[16 17] although this modality is not capable of tracking cellular and molecular dynamics in arthritic joints in situ. Recently, we and other groups have sought to establish methods for the intravital multiphoton imaging of joints in physiological and pathological conditions, and we have recently succeeded in visualising the dynamic behaviour of inflammatory cells in live murine joints (figure 2).

The most remarkable advantage of intravital fluorescent microscopy is its high spatiotemporal resolution with the observation of differently coloured respective cells. By using this intravital fluorescent joint imaging system, we could detect complex cellular interactions in arthritic joints in situ in the future, which could lead to the discovery of autoimmune inflammation exacerbation, bone-erosive mechanisms and pathogenic events in a murine arthritis model. For example, by using time-lapse fluorescent imaging, we will be able to analyse the very initial events regarding the onset of arthritis, such as immune/stromal intercellular crosstalk and inflammatory cell activation, which

would be critically useful for understanding pathogenic mechanisms of arthritis.

Different molecular-targeted biologics against RA could be tested using this new assay system to identify the critical point of control for therapeutics. Intravital imaging can also examine the time course of arthritis onset, which may be useful for identifying the pathogenic event of RA. Although the methodology has not yet been fully established, intravital fluorescent imaging of arthritic joints in the near future is sure to bring us a wealth of knowledge in the field of basic and clinical rheumatology. Due to the limited penetrance of visible light signals, it is hard to use fluorescent microscopy directly for elucidating human immunology (table 1). Nevertheless, recent developments on fluorescent endoscopy have enabled us to visualise local events in gastrointestinal tracts,[18] and such approach would be applicable also for arthroendoscopy in the future.

CLINICAL APPLICATION: NUCLEAR IMAGING FOR RA

Radioimaging modalities such as positron emission tomography (PET) could be beneficial for the evaluation of arthritis in humans. The system detects pairs of γ-rays emitted indirectly by a positron-emitting radionuclide tracer, which is introduced into the body on a biologically active molecule. Although the spatiotemporal resolution of PET is limited, the high signal-to-noise ratio enables us to detect phenomena deep inside the human body (table 1). Several previous PET studies have demonstrated localised joint inflammation in patients with RA with the use of ^{18}F-labelled fluorodeoxyglucose, an analogue of glucose analogue which is one of the most commonly used radioimaging probes for the detection of high-metabolising areas, such as inflammation and cancer.[19 20] The combined use of PET with other imaging modalities, such as MRI and CT, enables the visualisation of local synovial inflammation in RA. Recently, the dynamic behaviour of CD20$^+$ B cells in patients with RA has been detected using ^{124}I-labelled rituximab, a therapeutic anti-CD20 monoclonal antibody.[21] This kind of 'molecule-' or 'cell-targeted' radioimaging could become especially useful for analysing the pathophysiology of inflammation and bone erosion in RA.

The development and clinical application of biological agents have undoubtedly caused a paradigm shift in the therapeutics of RA, and several targets have been identified to date, such as tumour necrosis factor, interleukin (IL)-6 receptor, cytotoxic T lymphocyte antigen 4, IL-17 and Janus kinase 3. Several drugs have also been developed against tumour necrosis factor (eg, infliximab, etanercept, adalimumab, golimumab), and the next major consideration is the rational selection of appropriate therapeutics among these various drugs. Radiolabelled biological agents could be used to evaluate the involvement of the target molecule of interest in patients with RA and, thus, provide the clinician with information for making rational decisions in the selection of therapeutic agents. In addition, monitoring the status of targeted cytokines in patients may enable us to decide on the end point of the regimen. These developments will facilitate the creation of patient-specific regimens for patients with RA with the use of a wide array of therapeutic tools.

CONCLUSION

Major progress has been made recently in imaging techniques, and several tools for the visualisation of live biological systems in situ have become available. These tools must bring a paradigm shift in the field of basic and clinical rheumatology and lead to changes in the treatment of RA in the future.

Competing interests None.

Provenance and peer review Commissioned; externally peer reviewed.

REFERENCES

1. **Denk W**, Strickler JH, Webb WW. Two-photon laser scanning fluorescence microscopy. *Science* 1990;**248**:73–6.
2. **Cahalan MD**, Parker I, Wei SH, *et al.* Two-photon tissue imaging: seeing the immune system in a fresh light. *Nat Rev Immunol* 2002;**2**:872–80.
3. **Germain RN**, Miller MJ, Dustin ML, *et al.* Dynamic imaging of the immune system: progress, pitfalls and promise. *Nat Rev Immunol* 2006;**6**:497–507.
4. **Miller MJ**, Wei SH, Parker I, *et al.* Two-photon imaging of lymphocyte motility and antigen response in intact lymph node. *Science* 2002;**296**:1869–73.
5. **Garside P**, Brewer JM. Real-time imaging of the cellular interactions underlying tolerance, priming, and responses to infection. *Immunol Rev* 2008;**221**:130–46.
6. **Germain RN**, Bajénoff M, Castellino F, *et al.* Making friends in out-of-the-way places: how cells of the immune system get together and how they conduct their business as revealed by intravital imaging. *Immunol Rev* 2008;**221**:163–81.
7. **Bousso P**, Bhakta NR, Lewis RS, *et al.* Dynamics of thymocyte-stromal cell interactions visualized by two-photon microscopy. *Science* 2002;**296**:1876–80.
8. **Deane JA**, Hickey MJ. Molecular mechanisms of leukocyte trafficking in T-cell-mediated skin inflammation: insights from intravital imaging. *Expert Rev Mol Med* 2009;**11**:e25.
9. **Kreisel D**, Nava RG, Li W, *et al. In vivo* two-photon imaging reveals monocyte-dependent neutrophil extravasation during pulmonary inflammation. *Proc Natl Acad Sci USA* 2010;**107**:18073–8.
10. **Egen JG**, Rothfuchs AG, Feng CG, *et al.* Macrophage and T cell dynamics during the development and disintegration of mycobacterial granulomas. *Immunity* 2008;**28**:271–84.
11. **Chieppa M**, Rescigno M, Huang AY, *et al.* Dynamic imaging of dendritic cell extension into the small bowel lumen in response to epithelial cell TLR engagement. *J Exp Med* 2006;**203**:2841–52.
12. **Mazo IB**, Honczarenko M, Leung H, *et al.* Bone marrow is a major reservoir and site of recruitment for central memory CD8+ T cells. *Immunity* 2005;**22**:259–70.
13. **Ishii M**, Egen JG, Klauschen F, *et al.* Sphingosine-1-phosphate mobilizes osteoclast precursors and regulates bone homeostasis. *Nature* 2009;**458**:524–8.
14. **Klauschen F**, Ishii M, Qi H, *et al.* Quantifying cellular interaction dynamics in 3D fluorescence microscopy data. *Nat Protoc* 2009;**4**:1305–11.
15. **Ishii M**, Kikuta J, Shimazu Y, *et al.* Chemorepulsion by blood S1P regulates osteoclast precursor mobilization and bone remodeling in vivo. *J Exp Med* 2010;**207**:2793–8.
16. **Chen WT**, Mahmood U, Weissleder R, *et al.* Arthritis imaging using a near-infrared fluorescence folate-targeted probe. *Arthritis Res Ther* 2005;**7**:R310–7.
17. **Gompels LL**, Madden L, Lim NH, *et al. In vivo* fluorescence imaging of E-selectin: quantitative detection of endothelial activation in a mouse model of arthritis. *Arthritis Rheum* 2011;**63**:107–17.
18. **Urano Y**, Asanuma D, Hama Y, *et al.* Selective molecular imaging of viable cancer cells with pH-activatable fluorescence probes. *Nat Med* 2009;**15**:104–9.
19. **Kubota K**, Ito K, Morooka M, *et al.* FDG PET for rheumatoid arthritis: basic considerations and whole-body PET/CT. *Ann N Y Acad Sci* 2011;**1228**:29–38.
20. **Miese F**, Scherer A, Ostendorf B, *et al.* Hybrid (18)F-FDG PET-MRI of the hand in rheumatoid arthritis: initial results. *Clin Rheumatol* 2011;**30**:1247–50.
21. **Tran L**, Huitema AD, van Rijswijk MH, *et al.* CD20 antigen imaging with ^{124}I-rituximab PET/CT in patients with rheumatoid arthritis. *Hum Antibodies* 2011;**20**:29–35.

Chapter 10

Use of Intravital Microscopy and In Vitro Chemotaxis Assays to Study the Roles of Sphingosine-1-Phosphate in Bone Homeostasis

Taeko Ishii, Shunsuke Kawamura, Issei Nishiyama, Junichi Kikuta, and Masaru Ishii

Abstract

We describe a method to visualize the migration of osteoclast precursors within intact murine bone marrow in real time using intravital multiphoton microscopy. Conventionally, cell migration has been evaluated using in vitro systems, such as transmigration assays. Although these methods are convenient for quantification and are highly reproducible, these in vitro assay systems may not accurately reflect in vivo cellular behavior. In addition to in vitro analyses, recent technological progress in two-photon excitation-based laser microscopy has enabled the visualization of dynamic cell behavior deep inside intact living organs. Combining this imaging method with in vitro chemoattraction analyses, we have revealed that sphingosine-1-phosphate (S1P), a lipid mediator enriched in blood, bidirectionally controls the trafficking of osteoclast precursors between the circulation and bone marrow cavities via G protein-coupled receptors (GPCRs).

Key words: Intravital imaging, Multiphoton microscopy, Migration, Osteoclast precursor, S1P, S1PR1, S1PR2

1. Introduction

Bone is a dynamically regulated organ that continuously undergoes remodeling to maintain mineral homeostasis and structural robustness during growth and even in adulthood (1, 2). The balance between bone resorption by osteoclasts and bone formation by osteoblasts is finely regulated. During differentiation, osteoclasts and osteoblasts interact with and regulate each other (3). Recently, recruitment of osteoclast precursors was identified to

Alice Pébay and Kursad Turksen (eds.), *Sphingosine-1-Phosphate: Methods and Protocols*, Methods in Molecular Biology, vol. 874,
DOI 10.1007/978-1-61779-800-9_10, © Springer Science+Business Media, LLC 2012

be a critical control mechanism that maintains bone homeostasis (4–13). Osteoclasts are bone-resorbing, multinucleated giant cells that stem from mononuclear macrophage/monocyte-lineage hematopoietic precursors (2). These precursors are recruited at the correct time to appropriate sites for differentiation. We have developed a novel intravital multiphoton imaging system for visualizing the highly organized migration of osteoclast precursors between the bone marrow and blood vessels with high spatiotemporal resolution (13, 14). This new intravital imaging method showed that the bioactive lipid sphingosine-1-phosphate (S1P) controls the migratory behavior of osteoclast precursors in concert with various chemokines.

Multiphoton (usually two-photon) excitation-based laser microscopy has enabled visualization of living cells in intact living organs and analysis of their mobility and interactions quantitatively (15–18). The penetration depths of two-photon microscopy depend on the composition of the tissues. In contrast to soft tissues, such as the brain cortex, in which the penetration depth is 800–1,000 μm, accessing deep inside bone tissues is difficult. However, in the mouse parietal bone, the distance from the bone surface to the bone marrow cavity is only ~80–120 μm and within the range of two-photon microscopy. At this region, we can access the living bone marrow with minimal invasion. To observe cells with two-photon microscopy, they must be fluorescently labeled. We have used transgenic mice in which enhanced green fluorescent protein (EGFP) is expressed under the control of the promoter of CX_3CR1 (a CX_3CL1/fractalkine receptor) (19) or CSF1R (20), which are activated in monocytoid cells, including osteoclast precursors. Subsequently, we set up the platform to visualize the behavior of osteoclast precursors in a living body.

S1P transmits its signal through five 7-transmembrane receptors or G-protein-coupled receptors (GPCRs), named S1PR1 to S1PR5 (21). Among them, osteoclast precursors express S1PR1 and S1PR2 (13). S1PR1 activates Rac through G_i and promotes cell migration and intercellular connections, while S1PR2 conjugates $G_{12/13}$ and activates Rho pathways, which counteract S1PR1, thus inhibiting Rac activity (21). To clarify S1P function through each receptor, we intravenously injected FTY720 (22), an agonist for four of the five S1P receptors (all except S1PR2), a potent S1PR1 specific agonist SEW2871 (23), or a potent S1PR2 antagonist JTE013 (24) and then observed the mobility of osteoclast precursors.

In addition to this new imaging technique, to clarify the bidirectional chemotactic function of S1P concerning osteoclast precursors, we performed in vitro chemotaxis analysis with high and low concentrations of S1P using EZ-TAXIScan (14). This device enables visualization of the mobility of cells in real time in vitro.

In a high S1P environment, such as the blood circulation, S1PR1 is first activated and rapidly internalized, while S1PR2 is predominant. Osteoclast precursors enter bone marrow by chemorepulsion through S1PR2 and other chemokines attract them to the bone surface. In a low S1P environment, such as the bone marrow, as S1PR1 is restored on the cell surface, osteoclast precursors can recirculate from bone tissues to blood vessels through chemotaxis by the S1P gradient.

2. Materials

2.1. Multiphoton Microscopy

1. Upright microscope (DM6000B; Leica Microsystems) equipped with a 20× water immersion objective (HCX APO: numerical aperture (NA), 1.0; working distance)WD), 2.0 mm; Leica Microsystems) (see Note 1).
2. Femtosecond-pulsed infrared laser (MaiTai HP Ti:Sapphire laser; Spectra-Physics; see Note 2).
3. A non-descanned detector (NDD) that has 2–4 channels (see Note 3).
4. Customized microscope stage (see Note 4).
5. An environmental chamber in which anesthetized mice are warmed at 37°C by an air heater (see Note 5).

2.2. Anesthesia

1. Male or female CX_3CR1-EGFP knock-in mice (19), CSF1R(M-CSF receptor)-EGFP transgenic mice (20), osteoclast/monocyte-specific S1PR1-deficient mice, generated by crossing mice bearing conditional S1PR1 knockout alleles ($S1PR1^{loxP}$) (25) to transgenic mice expressing Cre under the Cd11b promoter (26) (see Note 6), and S1PR2-deficient mice (ref. 27; see Note 7).
2. Knockout mice are used with their wild-type (WT) littermates as the control.
3. Isoflurane (Escain).
4. Inhalation anesthesia apparatus (Baxter; 2.5% vaporized in an 80:20 mixture of O_2 and air).
5. Anesthesia box and mask.

2.3. Preparation of Mice

1. Custom-made stereotactic holder that can immobilize a mouse's head with fixing at three points—both ears and the foreteeth (Fig. 1).
2. Shaver and hair-removal lotion (Epilat).
3. Iris scissors and tweezers for mouse operation.
4. O-ring: a 1.5-mL microtube is cut into a 2-mm thick slice (see Note 8).

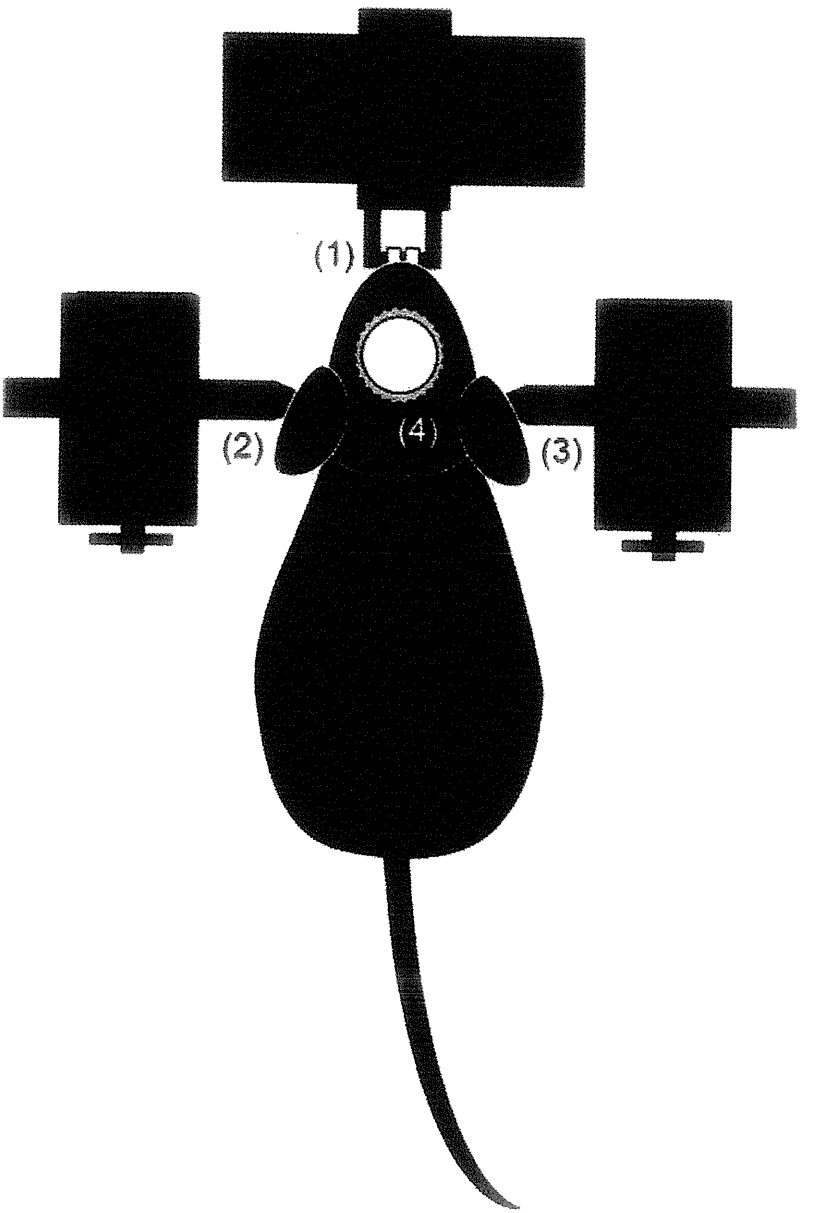

Fig. 1. Schematic illustration of how to fix a mouse on the stage. The mouse's head is immobilized with fixing at three points: foreteeth (1) and both ears (2 and 3). The O-ring is inserted into the incision of the skin and is filled with PBS (4).

[AU1]

5. Instant adhesive and petrolatum or Difloil grease.
6. Phosphate-buffered saline (PBS) immersion buffer, pH 7.4.

2.4. Staining of Blood Vessels

1. Angiographic agent: 2 mg/mL of 70-kDa Texas Red-conjugated dextran in PBS (see Note 9).
2. 29 or 30-G insulin syringes (Becton Dickinson) for intravenous injection.

2.5. Treatment with Reagents

1. FTY720 (3 mg/kg; Cayman Chemical) dissolved in a vehicle [PBS containing 5% acidified dimethylsulfoxide (DMSO) and 3% fatty acid-free bovine serum albumin (BSA)] or vehicle (22).

2. SEW2871 (5 mg/kg; Cayman Chemical) dissolved in a vehicle (PBS containing 5% acidified DMSO and 3% fatty acid-free BSA) or vehicle (23).
3. JTE013 (3 mg/kg; Tocris Bioscience) dissolved in a vehicle (PBS containing 5% acidified DMSO and 3% fatty acid-free BSA) or vehicle (24).
4. GST-RANKL (2 mg/kg, dissolved in PBS) (28).
5. 29- or 30-G insulin syringes (Becton Dickinson).
6. An indwelling needle: a 30-G needle attached to PE-10 tubing (Becton Dickinson).

2.6. Image Analysis

1. Imaging analysis software: Imaris (Bitplane) or Volocity (PerkinElmer).
2. After Effects (Adobe).

2.7. In Vitro Migration Assay

1. EZ-TAXIScan (Effector Cell Institute, GE HealthCare; see Note 10) containing "41 Glass," a small O-shaped ring, an EZ-TAXIScan chip, a rubber gasket, a holder base, wafer housing, a wafer clamp, a syringe guide, and a large O-shaped ring.
2. Sample loading tip attached to a plastic syringe (Becton Dickinson).
3. Microsyringe (10 μL; MS-E10MIC; Exmire).
4. 25-mm Thermanox plastic coverslip (Nunc; see Note 11).
5. Scissors and tweezers.
6. Serum-free Dulbecco's modified Eagle's medium (DMEM).
7. Serum-free alpha-minimum essential medium (αMEM) and αMEM with 10% fetal calf serum (FCS), containing 1% penicillin and streptomycin.
8. PBS, pH 7.4.
9. 0.02% EDTA in PBS.
10. Raw 264.7 cells (American Type Culture Collection, ATCC).
11. Male or female C57BL/6 mice (6-9 weeks old).
12. Syringe with 26-G needle.
13. Mouse recombinant macrophage colony-stimulating factor (M-CSF; 100 ng/mL; PeproTech).
14. Chemoattractant: S1P (10^{-6}, 10^{-7}, and 10^{-8} M; Enzo Life Sciences), dissolved in a vehicle (DMEM; see Note 12).
15. ImageJ software (National Institutes of Health, NIH), equipped with an add-on program, MT Track J.

3. Methods

3.1. Intravital Two-Photon Imaging

1. Start up the two-photon microscope and turn on the heater in the environmental chamber (see Note 13).
2. All the procedures on mice are performed under anesthesia (see Note 14). Shave the hair and apply hair-removal lotion on top of the mouse's head (see Note 15). Cut the skin minimally with iris scissors for insertion of the O-ring. Fix the O-ring on the parietal bone with adhesive and petrolatum or difloil grease (see Note 16), which prevents leakage of PBS and fills the O-ring.
3. Insert an indwelling needle into the tail vein to treat the mouse with reagents during observation.
4. Intravenously inject 100 μL of 2 mg/mL 70-kDa Texas Red-conjugated dextran in PBS (see Note 17).
5. Immobilize the mouse on the custom-made stereotactic holder as tightly as possible to avoid drift owing to respiration and pulsation (Fig. 1; see Note 18).
6. Focus on the bone marrow cavity at an appropriate depth and look through ocular lenses with the help of a mercury lamp. Change the light source from the mercury lamp to the Ti-Sapphire laser and the optical path to the NDD. Set the zoom ratio, *z*-positions, the interval time, and the duration time using observation software attached to the microscope (Fig. 2).
7. Inject 100 μL of each reagent per mouse.
8. Analyze images by measuring cellular velocities, migration lengths, and contact times using image processing and analysis software.

3.2. In Vitro Migration Assay

3.2.1. Bone Marrow-Derived M-CSF-Dependent Mononuclear Cells

1. Harvest bone marrow cells from C57BL/6 mice by flushing serum-free αMEM medium using a 26-G syringe.
2. Wash the harvested cells twice with αMEM containing FCS and culture the cells in αMEM containing FCS and 100 ng/mL M-CSF for 3 days.
3. Wash cells once with PBS and treat them with 0.02% EDTA in PBS.
4. Collect suspended cells and culture them in αMEM containing FCS and 100 ng/mL M-CSF for another 3 days.

3.2.2. Setting of EZ-TAXIScan

1. Place "41 Glass" in holder base. Drop DMEM in the center of the glass and place a coverslip over the liquid (see Note 19). Wipe off excess fluid, making sure no air bubbles are trapped between the glasses.

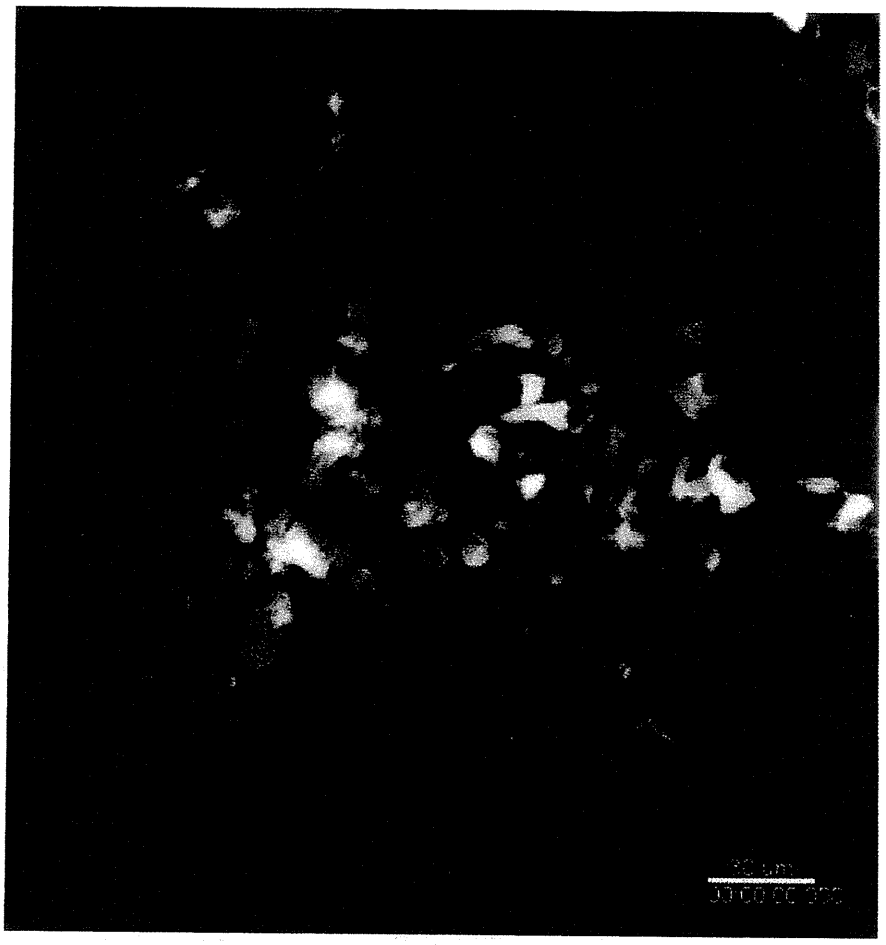

Fig. 2. Osteoclast precursors visualized by intravital two-photon imaging. Murine parietal bone of heterozygous Cx_3CR1-EGFP knock-in mice is visualized. CX_3CR1-EGFP-positive cells appear *green* in the bone marrow cavity. Collagen fibers in bone are detected by second-harmonic generation (*in blue*) and the blood vessels are visualized by 70-kDa dextran-conjugated Texas Red.

2. Place the small "O-shaped ring" on top of the wafer housing. Gently close the inner lever and fix the wafer housing.
3. Fill inside the wafer housing with 4 mL of DMEM.
4. Place the EZ-TAXIScan chip gently into the wafer housing (see Note 20), making sure no air bubbles are trapped. To protect the chip, place the rubber gasket beneath the wafer clamp. Place wafer clamp on wafer housing. Place the large O-shaped ring upside of the wafer housing. Gently close the outer lever (see Note 21).
5. Place the assembled device on top of the preheated EZ-TAXIScan microscope.

3.2.3. Alignment of Cells

1. Remove 1 mL of medium from the upper side of the holder.
2. Add 1 μL of cells (Raw 264.7 cells or bone-marrow derived M-CSF-dependent mononuclear cells) to the second chamber using a microsyringe with a syringe guide.

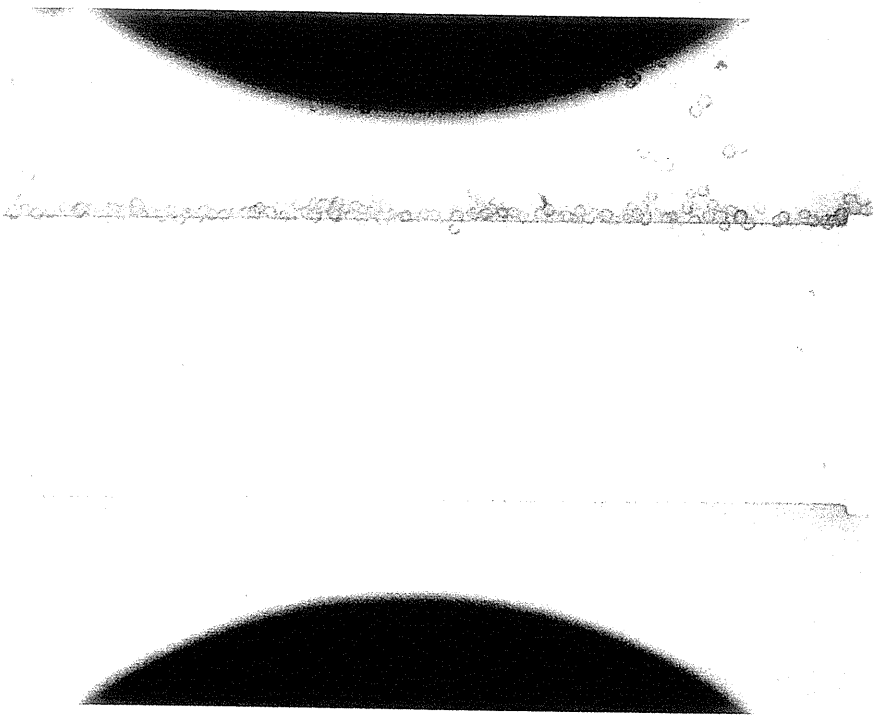

Fig. 3. Alignment of cells on one side of the EZ-TAXIScan chip before analysis. Before analysis of cell migration, cells should be aligned in the chamber on one side.

3. Remove 8–10 μL of medium from the third chamber using a microsyringe.
4. Monitor alignment of the cells on one side (Fig. 3).
5. Return the removed medium inside the holder.

3.2.4. Analysis of Chemotaxis

1. Begin image acquisition using 1-min intervals.
2. Add 1 ml of the chemoattractant (S1P: 10^{-6}, 10^{-7}, and 10^{-8} M) to the third chamber.
3. Sequential image data are processed and migration speeds and tracking distances are calculated using analysis software.

4. Notes

1. The two-photon microscopy setup is also available from other microscope manufacturers (Zeiss, Nikon, and Olympus). Regarding objective lenses, higher NA and longer WD should be desirable. Bone marrow can be observed through an inverted microscope.
2. A femtosecond-pulsed infrared laser is also available from Coherent (Chameleon).
3. The more channels the NDD has, the more colors can be detected.

4. As sufficient space is necessary to place a living mouse between the objective lens and the stage, we replaced the normal stage for the section with a customized one.
5. Because temperature is a critical factor for cell mobility, a decrease in body temperature of the animal must be prevented. Thus, we set up an environmental chamber, which can enclose the animal with the microscope stage and the objective lens.

[AU2]

6. Global S1PR1 deficiency causes embryonic lethally at e12.5 to e14.5 due to defective blood vessel development (29).
7. Although S1PR2-deficient mice suffer from auditory impairment due to vessel defects in the inner ear, they survive and reproduce (25).
8. The objective lens requires almost the same WD as that from the species. Additionally, as the objective lens is water immersible, the substance must be filled with the same refractive index as water between species and the lens. The O-ring works both as a spacer and a PBS reservoir.
9. We used a red dye in this protocol because the target cells express EGFP. If the target cells are red, dextran-conjugated fluorescein isothiocyanate (FITC) can be used. Far-red dyes, such as Qdot-650, can be an alternative if the NDD has a channel that can detect long-wavelength signals. As blood vessels inside the bone marrow cavity have relatively high permeability, dextran with molecular weights over 70 kDa should be used.
10. The EZ-TAXIscan is a visually accessible chemotactic chamber in which one compartment containing ligand (for example, S1P of various concentrations) and another compartment containing cells are connected by a microchannel. A stable concentration gradient of chemoattractant can be reproducibly formed and maintained through the channel without medium flow. Phase-contrast images of migrating cells are acquired at 1-min intervals.
11. 0.2 mm-thick cover slips coated with other reagents (such as collagen and fibronectin) can also be used.
12. Stock solutions of S1P are difficult to make. To accomplish this, S1P should be dissolved in BSA (4 mg/mL)-containing buffers or in other organic solvents with sonication or gentle warming (at 45–60°C).
13. It takes some time for the laser and the temperature to stabilize.
14. All animals must be handled according to institutional and national guidelines and regulations under an approved protocol.
15. Remove hair as much as possible to avoid hair coming into the visual field because it produces strong background autofluorescence.

16. Avoid glue contamination of the visual fields: some glues can produce autofluorescence.
17. With excretion of the dextran into urine, fluorescence fades after several hours. If necessary, additional dosage of the dye should be added.
18. Do not fasten too tightly because the animal can be hurt.
19. The coated side should be set upward.
20. The EZ-TAXIScan chip should be handled gently with tweezers. To protect it from drying, place it in a liquid at all times. After using, the EZ-TAXIScan chip should be sonicated and stored in 20–70% ethanol at room temperature. There are four types of EZ-TAXIScan chips with depths of 4, 5, 6, and 8 μm. The suitable size depends on the cell types. The 8-μm-depth chip should be used for Raw 264.7 cells and 5-μm-depth chip for bone marrow-derived M-CSF-dependent mononuclear cells.
21. Before setting up the assembled device, make sure no air bubbles remain inside the chamber. If air bubbles are present, remove them with the sample-loading tip attached to the plastic syringe.

Acknowledgment

This work was supported by Grants-in-Aid for Encouragement of Young Scientists (A) (22689030), for Scientific Research on Innovative Areas (22113007) and by a Funding Program for World-Leading Innovative R&D on Science and Technology (FIRST Program) from the Ministry of Education, Science, Sports and Culture of Japan, by a Grant-in-Aid for Research on Allergic Disease and Immunology (H21-010) from the Ministry of Health, Labor and Welfare of Japan, and by Grants from the International Human Frontier Science Program (CDA-00059/2009 and RGY-0077/2011).

References

1. Harada S, Rodan GA (2003) Control of osteoblast function and regulation of bone mass. Nature 423:349–355
2. Teitelbaum SL, Ross FP (2003) Genetic regulation of osteoclast development and function. Nat Rev Genet 4:638–649
3. Henriksen K et al (2009) Local communication on and within bone controls bone remodeling. Bone 44:1026–1033
4. Yu X et al (2003) Stromal cell-derived factor-1 (SDF-1) recruits osteoclast precursors by inducing chemotaxis, matrix metalloproteinase-9 (MMP-9) acrivity, and collagen transmigration. J Bone Miner Res 18:1404–1418
5. Wright LM et al (2005) Stromal cell-derived factor-1 binding to its chemokine receptor CXCR4 on precursor cells promotes the chemotactic recruitment, development and survival of human osteoclasts. Bone 36:840–853
6. Koizumi K et al (2009) Role of CX3CL1/fractalkine in osteoclast differentiation and bone resorption. J Immunol 183:7825–7831

7. Kim MS, Day CJ, Morrison NA (2005) MCP-1 is induced by receptor activator of nuclear factor-kB ligand, promotes human osteoclast fusion, and rescues granulocyte macrophage colony-stimulating fctor suppression of osteoclast formation. J Biol Chem 280: 16163–16169
8. Choi SJ et al (2000) Macrophage inflammatory protein 1-α is a potential osteoclast stimulatory factor in multiple myeloma. Blood 96: 671–675
9. Lean JM et al (2002) CCL9/MIP-1 gamma and its receptor CCR1 are the major chemokine ligand/receptor species expressed by osteoclasts. J Cell Biochem 87:386–393
10. Ha J et al (2010) CXC chemokine ligand 2 induced by receptor activator of NF-κB ligand enhances osteoclastogenesis. J Immunol 184: 4717–4724
11. Kwak HB et al (2008) Reciprocal cross-talk between RANKL and interferon-gamma-inducible protein 10 is responsible for bone-erosive experimental arthritis. Arthritis Rheum 58:1332–1342
12. Binder NB et al (2009) Estrogen-dependent and C-C chemokine receptor-2-dependent pathways determine osteoclast behavior in osteoporosis. Nat Med 15:417–424
13. Ishii M et al (2009) Sphingosine-1-phospate mobilizes osteoclast precursors and regulates bone homeostasis. Nature 458:524–528
14. Ishii M et al (2010) Chemorepulsion by blood S1P regulates osteoclast precursor mobilization and bone remodeling in vivo. J Exp Med 207:2793–2798
15. Cahalan MD et al (2002) Two-photon tissue imaging: seeing the immune system in a fresh light. Nat Rev Immunol 2:872–880
16. Germain RN et al (2006) Dynamic imaging of the immune system: progress, pitfalls and promise. Nat Rev Immunol 6:497–507
17. Wang BG, Konig K, Halbhuber KJ (2010) Two-photon microscopy of deep intravital tissues and its merits in clinical research. J Microsc 238:1–20
18. Germain RN et al (2008) Making friends in out-of-the-way places: how cells of the immune system get together and how they conduct their business as revealed by intravital imaging. Immunol Rev 221:163–181
19. Jung S et al (2000) Analysis of fractalkine receptro CX_3CR1 function by targeted deletion and green fluorescent protein reporter gene insertion. Mol Cell Biol 20:4106–4114
20. Burnett SH et al (2004) Conditional macrophage ablation in transgenic mice expressing a Fas-based suicide gene. J Leukoc Biol 75: 612–623
21. Rivera J, Proia RL, Olivera A (2008) The alliance of sphingosine-1-phosphate and its receptors in immunity. Nat Rev Immunol 8:753–763
22. Matloubian M et al (2004) Lymphocyte egress from thymus and peripheral lymphoid organs is dependent on S1P receptor 1. Nature 6972:355–360
23. Wer SH et al (2005) Sphingosine 1-phospate type 1 receptor agonism inhibits transendothelial migration of medullary T cells to lymphatic sinuses. Nat Immunol 12:1228–1235
24. Osaka M et al (2002) Enhancement of sphingosine 1-phosphate-induced migration of vascular endothelial cells and smooth muscle cells by an EDG-5 antagonist. Biochem Biophys Res Commun 299:483–487
25. Allende M et al (2003) G-protein-coupled receptor $S1P_1$ acts within endothelial cells to regulate vascular maturation. Blood 102: 3665–3667
26. Ferron M, Vacher J (2005) Targeted expression of Cre recombinase in macrophages and osteoclasts in transgenic mice. Genesis 41: 138–145
27. Kono M et al (2007) Deafness and stria vascularis defects in $S1P_2$ receptor-null mice. J Biol Chem 282:10690–10696
28. Tomimori Y et al (2009) Evaluation of pharmaceuticals with a novel 50-hour animal model of bone loss. J Bone Miner Res 24: 1194–1205
29. Liu Y et al (2000) Edg-1, the G-protein-coupled receptor for sphingosine-1-phosphate, is essential for vascular maturation. J Clin Invest 106:951–961

Rheumatol Int
DOI 10.1007/s00296-012-2397-1

ORIGINAL ARTICLE

Baseline anti-citrullinated peptide antibody (ACPA) titers and serum interleukin-6 (IL-6) levels possibly predict progression of bone destruction in early stages of rheumatoid arthritis (ERA)

Yukihiko Saeki · Eriko Kudo-Tanaka · Shiro Ohshima · Masato Matsushita · So-ichiro Tsuji · Yu-ichi Maeda · Maiko Yoshimura · Akane Watanabe · Yoshinori Katada · Yoshinori Harada · Kenji Ichikawa · Yasuo Suenaga · Yusuke Ohta · Shigeto Tohma · NHO iR-net Study Group

Received: 25 October 2011 / Accepted: 11 March 2012

Abstract A prospective study was made to seek for a convenient biomarker to predict progression of bone destruction (PBD) in early stages of rheumatoid arthritis (ERA). All participated patients had definite RA and their radiographic stages were mild less than stage II of the Steinbrocker classification, naïve for treatment of any DMARDs or corticosteroids. After the entry, they were treated according to the 2002 ACR management guideline for RA. The candidate biomarkers (RF-IgM, RF-IgG, CARF, ACPA, CRP, ESR, NTx, MMP-3, IL-6 and osteopontin) were measured at the entry. PBD was assessed radiographically by interval changes in the modified Sharp scores (ΔSHS) for 24 months. The associations between ΔSHS and baseline biomarkers were assessed statistically by multivariate regression analyses. Both the baseline ACPA and IL-6 levels correlated with PBD, suggesting that they could predict PBD in ERA.

Keywords Rheumatoid arthritis · Bone/joint destruction · Biomarker · Prediction · Anti-citrullinated peptide antibody (ACPA) · Interleukin-6 (IL-6)

Y. Saeki (✉) · S. Ohshima
Department of Clinical Research, National Hospital Organization (NHO) Osaka Minami Medical Center, 2-1 Kidohigashi-machi, Kawachinagano City, Osaka 586-8521, Japan
e-mail: saekiy@ommc-hp.jp

Y. Saeki · E. Kudo-Tanaka · S. Ohshima · M. Matsushita · S. Tsuji · Y. Maeda · M. Yoshimura · A. Watanabe
Department of Rheumatology, National Hospital Organization (NHO) Osaka Minami Medical Center, Osaka, Japan

Y. Katada · Y. Harada
Department of Allergology, National Hospital Organization (NHO) Osaka Minami Medical Center, Osaka, Japan

K. Ichikawa
Department of Rheumatology, NHO Hokkaido Medical Center, Sapporo, Japan

Y. Suenaga
Department of Rheumatology, NHO Beppu Medical Center, Beppu, Japan

Y. Ohta
Department of Rheumatology, NHO Minami-Okayama Medical Center, Okayama, Japan

S. Tohma
Department of Rheumatology, NHO Sagamihara Hospital, Sagamihara, Japan

Introduction

Rheumatoid arthritis (RA) is a systemic autoimmune disease of unknown origin characterized by chronic destructive polyarthritis which leads to disability and increased mortality. Although its etiology is unknown, the disease is thought to develop through three main processes such as autoimmunity, inflammation and subsequent bone resorption. On the other hand recent cumulative evidence suggests that early diagnosis and therapeutic interventions at the early stages of RA are important [1]. However, clinical course or prognosis of RA is not uniform but various. Therefore, the individual patient needs an optimal therapeutic strategy according to their prognosis. In order for this, the individual clinical course or prognosis should be predicted accurately. Although several candidate predictive biomarkers have been reported, none has been definite [2].

The aim of this prospective study was to seek for a useful biomarker measurable in the blood samples to

Published online: 29 March 2012